

MPP-2003-132  
 PSI-PR-04-02  
 SHEP-03-36  
 BNL-72033-2004-CP  
 hep-ph/0402212

## Determining the ratio of the $H^+ \rightarrow \tau\nu$ to $H^+ \rightarrow t\bar{b}$ decay rates for large $\tan\beta$ at the Large Hadron Collider

K.A. Assamagan<sup>a,\*</sup>, J. Guasch<sup>b,\*</sup>, S. Moretti<sup>c,\*</sup> and S. Peñaranda<sup>d,\*</sup>

<sup>a</sup>*Brookhaven National Laboratory, Upton NY 11792, USA*

<sup>b</sup>*Paul Scherrer Institut, CH-5232 Villigen PSI, Switzerland*

<sup>c</sup>*School of Physics and Astronomy, Southampton University, Highfield SO17 1BJ, UK*

<sup>d</sup>*Max-Planck-Institut für Physik, Föhringer Ring 6, D-80805 München, Germany*

### Abstract

We present results on the determination of the observable ratio  $R = BR(H^+ \rightarrow \tau^+\nu^-)/BR(H^+ \rightarrow t\bar{b})$  of charged Higgs boson decay rates as a discriminant quantity between Supersymmetric and non-Supersymmetric models. Simulation of measurements of this quantity through the analysis of the charged Higgs production process  $gb \rightarrow t\bar{b}H^+$  and relative backgrounds in the two above decay channels has been performed in the context of ATLAS. A  $\sim 12 - 14\%$  accuracy on  $R$  can be achieved for  $\tan\beta = 50, m_{H^\pm} = 300 - 500 \text{ GeV}$  and after an integrated luminosity of  $300 \text{ fb}^{-1}$ . With this precision measurement, the Large Hadron Collider (LHC) can easily discriminate between models for the two above scenarios, so long as  $\tan\beta > 20$ .

In this note we investigate the production of charged Higgs bosons in association with top quarks at the LHC, from the experimental and theoretical point of view, by studying hadronic ( $H^+ \rightarrow t\bar{b}$ ) and leptonic ( $H^+ \rightarrow \tau^+\nu$ ) decay signatures. The interest of this investigation is many-fold.

- The discovery of a charged Higgs boson will point immediately to the existence of some extension of the Standard Model (SM).
- The associated production of a charged Higgs boson with a top quark ( $pp \rightarrow H^+\bar{t} + X$ ) [1, 2] is only relevant at large values of  $\tan\beta^1$ , a regime where Higgs boson observables receive large Supersymmetric (SUSY) radiative corrections.

---

\*Electronic addresses: Ketevi.Adikle.Assamagan@cern.ch, jaume.guasch@psi.ch, stefano@hep.phys.soton.ac.uk, siannah@mppmu.mpg.de.

<sup>1</sup>It is in principle also relevant at very low values of  $\tan\beta$  (say,  $\lesssim 1$ ). In practise, this  $\tan\beta$  regime is excluded in the Minimal Supersymmetric Standard Model (MSSM) from the negative neutral Higgs search at LEP [3]. Hence, hereafter, we will refrain from investigating the low  $\tan\beta$  case.

- While SUSY radiative effects might be difficult to discern in the production cross-sections separately, they will appear neatly in the following relation between the two mentioned channels:

$$R \equiv \frac{\sigma(pp \rightarrow H^+\bar{t} + X \rightarrow \tau^+\nu t + X)}{\sigma(pp \rightarrow H^+\bar{t} + X \rightarrow t\bar{b} + X)}. \quad (1)$$

- In fact, in the ratio of (1), the dependence on the production mode (and on its large sources of uncertainty deriving from parton luminosity, unknown QCD radiative corrections, scale choices, etc.) cancels out:

$$R = \frac{BR(H^+ \rightarrow \tau^+\nu)}{BR(H^+ \rightarrow t\bar{b})} = \frac{\Gamma(H^+ \rightarrow \tau^+\nu)}{\Gamma(H^+ \rightarrow t\bar{b})}. \quad (2)$$

From these remarks it is clear that the quantity  $R$  is extremely interesting both experimentally and theoretically in investigating the nature of Electro-Weak Symmetry Breaking (EWSB).

In the MSSM, Higgs boson couplings to down-type fermions receive large quantum corrections, enhanced by  $\tan\beta$ . These corrections have been resummed to all orders in perturbation theory with the help of the effective Lagrangian formalism for the  $t\bar{b}H^+$  vertex [4, 5]. The  $b$ -quark Yukawa coupling,  $h_b$ , is related to the corresponding running mass at tree level by  $h_b = m_b/v_1$ . Once radiative corrections are taken into account, due to the breaking of SUSY, this relation is modified to  $m_b \equiv h_b v_1 (1 + \Delta m_b)$  [4, 5], where  $v_i$  is the Vacuum Expectation Value (VEV) of the Higgs doublet  $H_i$  and  $\Delta m_b$  is a non-decoupling quantity that encodes the leading higher order effects. Similarly to the  $b$ -quark case, the relation between  $m_\tau$  and the  $\tau$ -lepton Yukawa coupling,  $h_\tau$ , is also modified by quantum corrections,  $\Delta m_\tau$ . We adopt in our analysis the effective Lagrangian approach by relating the fermion mass to the Yukawa coupling via a generic  $\Delta m_f$  ( $f = b, \tau$ ),

$$h_f = \frac{m_f(Q)}{v_1} \frac{1}{1 + \Delta m_f} = \frac{m_f(Q)}{v \cos\beta} \frac{1}{1 + \Delta m_f} \quad (v = (v_1^2 + v_2^2)^{1/2}, \quad \tan\beta = \frac{v_1}{v_2}), \quad (3)$$

in which the resummation of all possible  $\tan\beta$  enhanced corrections of the type  $(\alpha_s \tan\beta)^n$  is included [4, 5]. The leading part of the (potentially) non-decoupling contributions proportional to soft-SUSY-breaking trilinear scalar couplings ( $A_f$ ) can be absorbed in the definition of the effective Yukawa coupling at low energies and only subleading effects survive [5]. Therefore, the expression (3) contains all (potentially) large leading radiative effects. The SUSY-QCD contributions to  $\Delta m_b$  are proportional to the Higgsino mass parameter  $\Delta m_b \sim \mu$ , while the leading SUSY-EW contributions behave like  $\Delta m_b \sim \mu A_t$  [6]. Thus, they can either enhance or screen each other, depending on the sign of  $A_t$ . It is precisely these effects that will allow us to distinguish between different Higgs mechanisms of EWSB. For example, the analysis of these corrections in the ratio of neutral Higgs boson decay rates,  $R' = BR(H \rightarrow b\bar{b})/BR(H \rightarrow \tau^+\tau^-)$ , revealed large deviations from the SM values for several MSSM parameter combinations [6]. Extensive theoretical analyses of

one-loop corrections to both neutral and charged Higgs boson decays have been performed in [6–17]. We now explore the one-loop MSSM contributions to the ratio of the branching ratios ( $BR$ s) of a charged Higgs boson  $H^\pm$  in (2), which at leading order (and neglecting kinematical factors) is given by  $R = h_\tau^2/3h_b^2$  in the large  $\tan\beta$  limit. The SUSY corrections to the  $H^+t\bar{b}$  vertex entering the decay processes  $t \rightarrow H^+b$  and  $H^+ \rightarrow t\bar{b}$  have been analysed in [7–10], where it was shown that they change significantly the Tevatron limits on  $m_{H^\pm}$  [10]. They were further explored in the production process  $pp(p\bar{p}) \rightarrow H^\pm t\bar{b}$  at LHC and Tevatron in [11–13, 18], where they were shown to shift significantly the prospects for discovery of a charged Higgs boson at both colliders.

Here, we have performed a detailed phenomenological analysis for the LHC of charged Higgs boson signatures, by using the subprocess  $g\bar{b} \rightarrow H^+\bar{t}$ . The QCD corrections to this channel are known to next-to-leading (NLO) [19]. However, we have normalised our production cross-section to the LO result, for consistency with the tree-level treatment of the backgrounds<sup>2</sup>. In our simulation, we have let the top quarks decay through the SM-like channel  $t \rightarrow W^+b$ . In the hadronic decay channel of the charged Higgs boson ( $H^+ \rightarrow t\bar{b}$ ) we require one of the two  $W$ 's emerging from the decay chain  $H^+\bar{t} \rightarrow (t\bar{b})\bar{t} \rightarrow (W^+b)\bar{b}(\bar{b}W^-)$  to decay leptonically, to provide an efficient trigger, while the other  $W$  is forced to decay hadronically, since this mode provides the largest rate and in order to avoid excessive missing energy. The  $\tau$ -lepton in the  $H^+ \rightarrow \tau^+\nu$  decay mode is searched for through hadronic one- and multi-prong channels. In summary, the experimental signatures of the two production channels under investigation are ( $l = e, \mu$ ):

$$pp(g\bar{b}) \rightarrow H^+\bar{t} \rightarrow (\tau^+\nu)\bar{t} \rightarrow \tau^+\nu(jj\bar{b}), \quad (4)$$

$$pp(g\bar{b}) \rightarrow H^+\bar{t} \rightarrow (t\bar{b})\bar{t} \rightarrow (jj[l\nu]b)\bar{b}(l\nu[jj]\bar{b}). \quad (5)$$

(In the numerical analysis we always combine the signals in (4) and (5) with their charged-conjugated modes.)

The Monte Carlo (MC) simulation has been performed using PYTHIA (v6.217) [20] for the signal and most of the background processes. (We have cross-checked the signal cross-section with [19].) We have used HDECAY [21] for the Higgs boson decay rates. One of the background processes (the single-top one: see below) has been generated with TopRex [22] with a custom interface to PYTHIA. We have used ATLFast [23] for the detector simulation. (Further details of the detector can be found in [24, 25].) We have adopted the CTEQ5L [26] parton distribution functions in their default PYTHIA v6.217 setup and we have used running quark masses derived from the pole values  $m_t^{\text{pole}} = 175 \text{ GeV}$  and  $m_b^{\text{pole}} = 4.62 \text{ GeV}$ . The TAUOLA [27–29] package was interfaced to the PYTHIA event generator for treatment of the  $\tau$ -lepton polarisation.

The leptonic decay channel of the charged Higgs boson provides the best probe for the detection of such a state at the LHC. In fact, it turns out that despite the small branching

---

<sup>2</sup>In all the analysis we disregard the subleading QCD and SUSY corrections which affect the signal and the background, and will take only into account the leading SUSY corrections to the signal cross-section, which are absent in the background processes.

	$m_{H^\pm} = 350$	$m_{H^\pm} = 500$	$t\bar{t}$	$W^\pm t$
$\sigma \times BR$	99.9 fb	30.7 fb	79.1 pb	16.3 pb
Events	29958	9219	$2.3 \times 10^6$	$4.89 \times 10^5$
Events after cuts	174	96	17	3
Efficiency	0.6%	1%	$8 \times 10^{-6}$	$6 \times 10^{-6}$
$S/B$	7.9	4.4		
$S/\sqrt{B}$	37.1	20.5		
Poisson	23.1	14.6		

Table 1: The signal and background cross-sections, the number of events before cuts, the number of events after all cuts, the total efficiency, the signal-to-background ratios ( $S/B$ ), and the signal significances (Gaussian and Poisson) for the detection of the charged Higgs in the  $\tau\nu$  channel at the LHC, for  $300 \text{ fb}^{-1}$  integrated luminosity and  $\tan\beta = 50$ .

ratio  $BR(H^+ \rightarrow \tau^+\nu)$ , the  $\tau$ -lepton affords an efficient trigger to observe this channel. The production rates  $\sigma \times BR(H^+ \rightarrow \tau^+\nu) \times BR(W \rightarrow jj)$  are shown in Tab. 1. The main background processes in this channel are: top-pair production with one of the  $W$ 's decaying into  $\tau\nu$  ( $gg \rightarrow t\bar{t} \rightarrow jj b \tau\nu\bar{b}$ ) and  $W^\pm t$  associated production ( $g\bar{b} \rightarrow W^+\bar{t} \rightarrow \tau^+\nu\bar{t}$ ).

We have used the following trigger conditions: hadronic  $\tau$ -jet ( $p_T^\tau > 30 \text{ GeV}$ ); a  $b$ -tagged jet ( $p_T^b > 30 \text{ GeV}$ ) and at least two light jets ( $p_T^j > 30 \text{ GeV}$ ). We apply afterwards a  $b$ -jet veto to reject the  $t\bar{t}$  QCD background. As there is no isolated lepton (electron or muon) in the final state, the observation of this channel requires a multi-jet trigger with a  $\tau$ -trigger. After reconstructing the jet-jet invariant mass  $m_{jj}$  and retaining the candidates consistent with the  $W$ -boson mass,  $|m_W - m_{jj}| < 25 \text{ GeV}$ , the jet four-momenta are rescaled and the associated top quark is reconstructed by minimising  $\chi^2 \equiv (m_{jjb} - m_t)^2$ . Subsequently, a sufficiently high threshold on the  $p_T$  of the  $\tau$ -jet is required,  $p_T^\tau > 100 \text{ GeV}$ . The background events satisfying this cut need a large boost from the  $W$ -boson. This results in a small azimuthal opening angle  $\Delta\phi$  between the  $\tau$ -jet and the missing transverse momentum,  $\cancel{p}_T$ . For background suppression we then have the cut  $\Delta\phi(\cancel{p}_T, p_T^\tau) > 1$ . Besides, the missing transverse momentum is harder for the signal than for the background while the differences between their distributions in azimuthal angle and missing transverse momentum increase with increasing  $m_{H^\pm}$ . These effects are well cumulated in the transverse mass,  $m_T = \sqrt{2p_T^\tau \cancel{p}_T [1 - \cos(\Delta\phi)]}$ , which provides good discrimination between the signal and the backgrounds, as shown in Fig. 1. (Further details of this kind of studies are available in [24, 25].) The discussed set of cuts reduces the total background by six orders of magnitude while the signal is only suppressed by two orders. The production rates and total detection efficiency (including detector acceptance,  $b$ - and  $\tau$ -identification, pileup and the effect of cuts) are also shown in Tab. 1 for an integrated luminosity of  $300 \text{ fb}^{-1}$ . We can see that the signal rates are large enough to indeed consider  $H^+ \rightarrow \tau\nu$  a *golden channel* for the  $H^+$  discovery at large  $\tan\beta$ .

The production rates  $\sigma \times BR(H^+ \rightarrow t\bar{b}) \times BR(W^+W^- \rightarrow jj\nu\bar{\nu})$  are shown in Tab. 2.

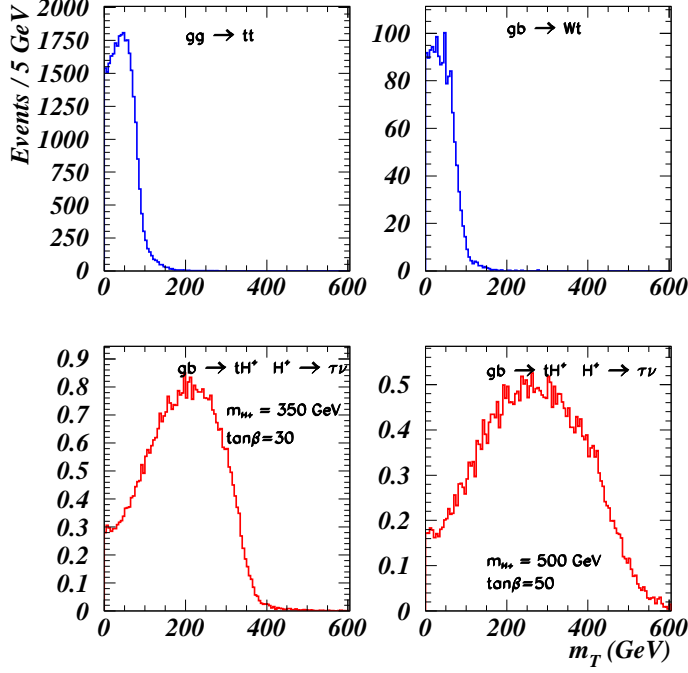


Figure 1: Transverse mass  $m_T$  distribution for signal and total background taking into account the polarisation of the  $\tau$ -lepton, for an integrated luminosity of  $30 \text{ fb}^{-1}$ . A final cut  $m_T > 200 \text{ GeV}$  was used for the calculations of the signal-to-background ratios and for the signal significances.

The decay mode  $H^\pm \rightarrow tb$  has large QCD backgrounds at hadron colliders that come from  $t\bar{t}q$  production with  $t\bar{t} \rightarrow WbWb \rightarrow l\nu bjjb$ . However, the possibility of efficient  $b$ -tagging has considerably improved the situation [30–32]. We search for an isolated lepton ( $p_T^e > 20 \text{ GeV}$ ,  $p_T^\mu > 8 \text{ GeV}$ ), three  $b$ -tagged jets ( $p_T^b > 30 \text{ GeV}$ ) and at least two non  $b$ -jets ( $p_T^j > 30 \text{ GeV}$ ). We retain the jet-jet combinations whose invariant masses are consistent with the  $W$ -boson mass,  $|m_W - m_{jj}| < 25 \text{ GeV}$ , then we use the  $W$ -boson mass constraint to find the longitudinal component of the neutrino momentum in  $W^\pm \rightarrow l\nu$ , by assuming that the missing transverse momentum belongs only to the neutrino. Subsequently, the two top quarks entering the  $H^+\bar{t} \rightarrow (t\bar{b})\bar{t} \rightarrow (jj[l\nu]b)\bar{b} (l\nu[jj]\bar{b})$  decay chain are reconstructed, retaining the pairing whose invariant masses  $m_{l\nu b}$  and  $m_{jjb}$  minimise  $\chi^2 \equiv (m_t - m_{l\nu b})^2 + (m_t - m_{jjb})^2$ . The remaining  $b$ -jet can be paired with either top quark to give two charged Higgs candidates, one of which leads to a combinatorial background. The expected rates for signal and background (after the mentioned decays) are shown in Tab. 2. (This analysis is presented extensively in [24, 25].)

At this point, we have two charged Higgs candidates:  $t_1b_3$  or  $t_2b_3$ . Assuming that the charged Higgs is discovered through the  $H^\pm \rightarrow \tau\nu$  channel and its mass determined from the  $\tau\nu$  transverse mass distribution [24, 25], the correct charged Higgs candidate in the  $tb$  channel can be selected by using the measured  $m_{H^\pm}$  as a constraint. This is done

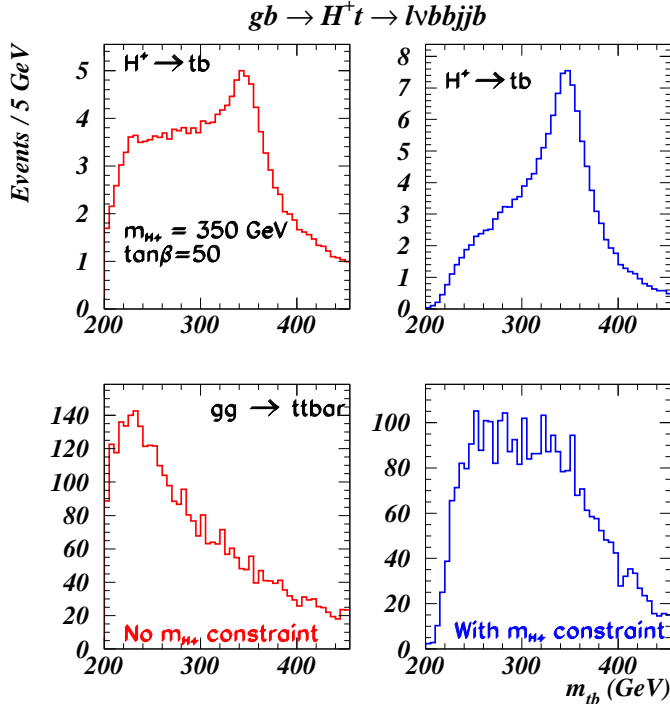


Figure 2: The signal and the background distributions for the reconstructed invariant mass  $m_{tb}$  of  $m_{H^\pm} = 350$  GeV,  $\tan\beta = 50$  and an integrated luminosity of  $30 \text{ fb}^{-1}$ . Assuming that the charged Higgs is discovered in the  $H^\pm \rightarrow \tau\nu$  channel, one can use  $m_{H^\pm}$  as a constraint to reduce the combinatorial background: this is shown on the right plots.

by selecting the candidate whose invariant mass is closest to the measured charged Higgs mass:  $\chi^2 = (m_{tb} - m_{H^\pm})^2$ . The signal distribution for the reconstructed invariant mass  $m_{tb}$  for a charged Higgs boson weighing 350 GeV, with  $\tan\beta = 50$  and after integrated luminosity of  $30 \text{ fb}^{-1}$ , is shown in Fig. 2. We can see that for the  $H^+ \rightarrow t\bar{b}$  decay some irreducible combinatorial noise still appears even when the  $m_{H^\pm}$  constraint is included. In addition, for the background, we have found that the  $m_{H^\pm}$  constraint reshapes the distributions in  $gg \rightarrow t\bar{t}X$  in such a way that no improvement in the signal-to-background ratio and signal significance is further observed. Finally, recall that the knowledge of the shape and the normalisation of the reshaped background would be necessary for the signal extraction. For these reasons, we did not use the  $m_{H^\pm}$  constraint for the results shown in this work. The subtraction of the background can then be done by fitting the side bands and extrapolating in the signal region which will be known from the  $m_{H^\pm}$  determination in the  $H^\pm \rightarrow \tau\nu$  channel: however, this would be possible only for Higgs masses above 300 GeV – see Fig. 2. The signal and background results are summarised in Tab. 2 at an integrated luminosity of  $300 \text{ fb}^{-1}$  for different values of  $m_{H^\pm}$  and  $\tan\beta = 50$ . It is shown that it is difficult to observe  $H^\pm$  signals in this channel above  $\sim 400$  GeV, even with the  $m_{H^\pm}$  constraint. For masses above  $m_{H^\pm} \sim 400$  GeV the signal significance can be enhanced by using the kinematics of the three-body production process  $gg \rightarrow H^\pm t\bar{b}$  [11–13, 30–32].

We assume a theoretical uncertainty of 5% on the branching ratios,  $BR$ s. Previous AT-

	$m_{H^\pm} = 350$	$m_{H^\pm} = 500$	$t\bar{t}q$
$\sigma \times BR$	248.4 fb	88 fb	85 pb
Events	74510	26389	$2.55 \times 10^7$
Events after cuts	2100	784	59688
Efficiency	2.8%	3%	0.2%
$S/B$	0.035	0.013	
$S/\sqrt{B}$	8.6	3.2	

Table 2: The signal and background cross-sections, the number of events before cuts, the number of events after all cuts, total efficiency,  $S/B$ , and the signal significances for the detection of the charged Higgs in the  $t\bar{b}$  channel at the LHC, for  $300 \text{ fb}^{-1}$  integrated luminosity and  $\tan\beta = 50$ .

LAS studies have shown the residual  $gg \rightarrow t\bar{t}$  shape and normalisation can be determined to 5% [24, 25]. The scale uncertainties on jet and lepton energies are expected to be of the order 1% and 0.1% respectively [24, 25]. As explained above, for  $m_{H^\pm} > 300 \text{ GeV}$ , the side band procedure can be used to subtract the residual background under the  $H^+ \rightarrow t\bar{b}$  signal: we assume also a 5% uncertainty in the background subtraction method. Thus, the statistical uncertainties can be estimated as  $\sqrt{1/S}$ . The uncertainty in the ratio  $R$  are dominated by the reduced knowledge of the background shape and rate in the  $H^+ \rightarrow t\bar{b}$  channel. The cumulative results for the two channels are summarised in Tab. 3 at an integrated luminosity of  $300 \text{ fb}^{-1}$ . Here, the final result for the ratio  $R$  is obtained by correcting the visible production rates after cuts for the total detection efficiency in Tabs. 1 and 2 and by the decay  $BR$ s of the  $W$ -bosons. The simulation shows that the above mentioned ratio can be measured with an accuracy of  $\sim 12 - 14\%$  for  $\tan\beta = 50$ , for  $m_{H^\pm} = 300 - 500 \text{ GeV}$  and at an integrated luminosity of  $300 \text{ fb}^{-1}$ .

We turn now to the impact of the SUSY radiative corrections. Their role is twofold. Firstly, by changing the value of the Yukawa coupling they change the value of the observable  $R$ . Secondly, they can change the value of the production cross-section  $\sigma(pp \rightarrow H^+\bar{t} + X)$ , hence shifting significantly (by as much as 100 GeV) the range of charged Higgs masses accessible at the LHC [11–13].

To explore the second consequence, we rely on the fact that the bulk of the SUSY corrections to the production cross-section is given by the Yukawa coupling redefinition in (3) [11–13, 19]. By neglecting the kinematic effects, taking the large  $\tan\beta$  limit and assuming that the dominant decay channel of the charged Higgs boson is  $H^+ \rightarrow t\bar{b}$  (large mass limit), we can estimate the corrected production rates. For simplicity, we show only the contributions to  $\Delta m_b$ , since they are the dominant ones:

$$\begin{aligned} \sigma^{\text{corr}}(g\bar{b} \rightarrow H^+\bar{t} \rightarrow t\bar{b}\bar{t}) &= \sigma^{\text{corr}}(g\bar{b} \rightarrow H^+\bar{t}) \times BR^{\text{corr}}(H^+ \rightarrow t\bar{b}) \simeq \frac{\sigma^0(g\bar{b} \rightarrow H^+\bar{t})}{(1 + \Delta m_b)^2}, \\ \sigma^{\text{corr}}(g\bar{b} \rightarrow H^+\bar{t} \rightarrow \tau^+\nu\bar{t}) &= \sigma^{\text{corr}}(g\bar{b} \rightarrow H^+\bar{t}) \times \frac{\Gamma(H^+ \rightarrow \tau^+\nu)}{\Gamma^{\text{corr}}(H^+ \rightarrow t\bar{b})} \end{aligned}$$

	$m_{H^\pm} = 350$	$m_{H^\pm} = 500$
Signals $\tau\nu/tb$	174 / 2100 = 0.08	96 / 784 = 0.12
Signals (corrected) $\tau\nu/tb$	0.18	0.16
Systematics unc.	$\sim 9\%$	$\sim 9\%$
Total unc.	12%	14%
Theory	0.18	0.16

Table 3: Experimental determination of the ratio (1) for  $300 \text{ fb}^{-1}$  and  $\tan\beta = 50$ . Shown are: the signal after cuts, the signal after correcting for efficiencies and branching ratios, the systematic uncertainty, the total combined uncertainty, and the theoretical prediction (without SUSY corrections).

$$\simeq \frac{\sigma^0(g\bar{b} \rightarrow H^+\bar{t})}{(1 + \Delta m_b)^2} \times \frac{\Gamma(H^+ \rightarrow \tau^+\nu)}{\Gamma^0(H^+ \rightarrow t\bar{b}) \times \frac{1}{(1+\Delta m_b)^2}}. \quad (6)$$

This very simple exercise shows that the production rate in the  $\tau$ -channel is fairly independent of the SUSY radiative corrections and therefore the tree-level analysis performed above can (to a very good approximation) be used for our original purposes. Actually, once we take into account kinematical effects, the  $\tau$ -channel will receive small (negative) corrections in the low charged Higgs mass range. However, in this range,  $BR(H^+ \rightarrow \tau^+\nu)$  is quite large and one should not fear to lose the signal. Quite the opposite, the hadronic  $t\bar{b}$  production channel receives large radiative corrections. These corrections can be either positive (enhancing the signal, and therefore the significance in Tab. 2) or negative (reducing it, possibly below observable levels)<sup>3</sup>. In Fig. 3a, we show the discussed enhancement/suppression factors as a function of  $\tan\beta$  for  $m_{H^\pm} = 350 \text{ GeV}$  and a SUSY mass spectrum defined as SPS4 of the *Snowmass Points and Slopes* in [33], but choosing different scenarios for the sign of  $\mu$  and  $A_t$ <sup>4</sup>. (It is worth noting that the production rate for the  $t\bar{b}$ -channel can be enhanced by a factor larger than 3 in some SUSY scenarios, which would enhance significantly the corresponding signal thus overcoming the low signal-to-background ratio of this channel.)

We now turn our attention to the observable under analysis. Fig. 3b shows the prediction for the ratio  $R$  as a function of  $\tan\beta$  for the SPS4 scenario with a charged Higgs mass of  $m_{H^\pm} = 350 \text{ GeV}$ . The value of  $R$  only depends on  $m_{H^\pm}$  through kinematical factors and the dependence is weak for  $m_{H^\pm} \gtrsim 300 \text{ GeV}$ . In this figure, we also show the experimental determination carried out as before and repeated for each SUSY setup. From Fig. 3b it is clear that radiative SUSY effects are visible at the LHC at a large significance. In particular, the  $\mu < 0$  scenarios can easily be discriminated, while the  $\mu > 0$  ones will be more difficult to establish, due to the lower signal rate of the hadronic channel. This feature then also allows for a measurement of the sign of the  $\mu$  parameter. In contrast, since radiative corrections are independent of the overall SUSY scale, the observable  $R$  cannot provide us

<sup>3</sup>Alternative analyses may permit the signal to be seen even in this unfavourable case [11–13].

<sup>4</sup>The SPS4 spectrum is affected by moderate SUSY radiative corrections.



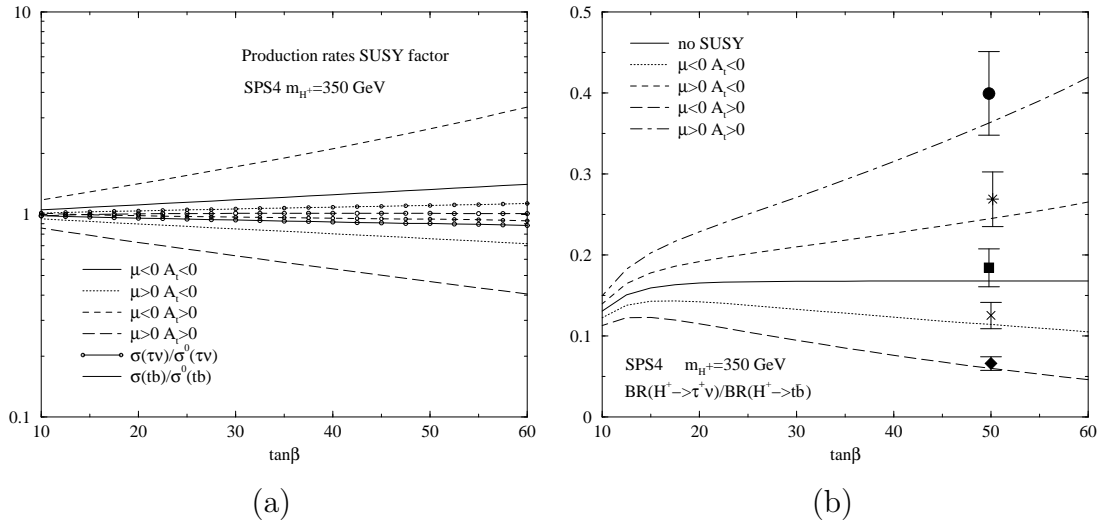


Figure 3: a) Production rates enhancement/suppression factors for the  $\tau$  and the  $tb$  channels; b) the SUSY correction to the rate (2). Plots as functions of  $\tan\beta$  for  $m_{H^\pm} = 350$  GeV and a SUSY spectrum as in SPS4, but for different choices of the signs of  $\mu$  and  $A_t$ . Shown is also the experimental determination for each scenario.

with an estimation of the typical mass of SUSY particles. Nonetheless, the information obtained in other production channels (e.g., neutral Higgs bosons or SUSY particles direct production) can be used to perform precision tests of the MSSM.

To summarise, we have used the observable  $R \equiv \frac{\sigma(pp \rightarrow H^+ \bar{l} + X \rightarrow \tau^+ \nu l + X)}{\sigma(pp \rightarrow H^+ \bar{l} + X \rightarrow tb + X)} = \frac{BR(H^+ \rightarrow \tau^+ \nu^-)}{BR(H^+ \rightarrow tb)}$  to discriminate between SUSY and non-SUSY Higgs models. This quantity is a theoretically *clean* observable. The experimental uncertainties that appear in this ratio have been analysed in details through detailed phenomenological simulations. In the MSSM,  $R$  is affected by quantum contributions that do not decouple even in the heavy SUSY mass limit. We have quantitatively shown that an LHC measurement of  $R$  can give clear evidence for or against the SUSY nature of charged Higgs bosons.

## Acknowledgements

KAA, JG and SM wish to thank the Les Houches workshop organisation and participants for the warm atmosphere of the workshop. JG acknowledges financial support from the Les Houches workshop organisation and SM from The Royal Society (London, UK).

## References

- [1] J. F. Gunion, Phys. Lett. **B322**, 125–130 (1994), hep-ph/9312201.
- [2] V. D. Barger, R. J. N. Phillips and D. P. Roy, Phys. Lett. **B324**, 236–240 (1994), hep-ph/9311372.

- [3] The LEP Higgs Working Group, *Searches for the neutral Higgs bosons of the MSSM: Preliminary combined results using LEP data collected at energies up to 209-GeV*, hep-ex/0107030.
- [4] M. Carena, D. Garcia, U. Nierste and C. E. M. Wagner, Nucl. Phys. **B577**, 88–120 (2000), hep-ph/9912516.
- [5] J. Guasch, P. Häfliger and M. Spira, Phys. Rev. **D68**, 115001 (2003), hep-ph/0305101.
- [6] J. Guasch, W. Hollik and S. Peñaranda, Phys. Lett. **B515**, 367–374 (2001), hep-ph/0106027.
- [7] J. Guasch, R. A. Jiménez and J. Solà, Phys. Lett. **B360**, 47–56 (1995), hep-ph/9507461.
- [8] J. A. Coarasa, D. Garcia, J. Guasch, R. A. Jiménez and J. Solà, Eur. Phys. J. **C2**, 373–392 (1998), hep-ph/9607485.
- [9] J. A. Coarasa, D. Garcia, J. Guasch, R. A. Jiménez and J. Solà, Phys. Lett. **B425**, 329–336 (1998), hep-ph/9711472.
- [10] J. Guasch and J. Solà, Phys. Lett. **B416**, 353–360 (1998), hep-ph/9707535.
- [11] A. Belyaev, D. Garcia, J. Guasch and J. Solà, Phys. Rev. **D65**, 031701 (2002), hep-ph/0105053.
- [12] A. Belyaev, D. Garcia, J. Guasch and J. Solà, JHEP **06**, 059 (2002), hep-ph/0203031.
- [13] A. Belyaev, J. Guasch and J. Solà, Nucl. Phys. Proc. Suppl. **116**, 296 (2003), hep-ph/0210253.
- [14] M. Carena, H. E. Haber, H. E. Logan and S. Mrenna, Phys. Rev. **D65**, 055005 (2002), hep-ph/0106116, [Erratum-ibid. D **65** (2002) 099902].
- [15] A. M. Curiel, M. J. Herrero, D. Temes and J. F. De Troconiz, Phys. Rev. **D65**, 075006 (2002), hep-ph/0106267.
- [16] M. J. Herrero, S. Peñaranda and D. Temes, Phys. Rev. **D64**, 115003 (2001), hep-ph/0105097.
- [17] H. E. Haber, M. J. Herrero, H. E. Logan, S. Peñaranda, S. Rigolin and D. Temes, Phys. Rev. **D63**, 055004 (2001), hep-ph/0007006.
- [18] M. Guchait and S. Moretti, JHEP **01**, 001 (2002), hep-ph/0110020.
- [19] T. Plehn, Phys. Rev. **D67**, 014018 (2003), hep-ph/0206121.

- [20] T. Sjostrand et al., *Comput. Phys. Commun.* **135**, 238–259 (2001), [hep-ph/0010017](#).
- [21] A. Djouadi, J. Kalinowski and M. Spira, *Comput. Phys. Commun.* **108**, 56–74 (1998), [hep-ph/9704448](#).
- [22] S. R. Slabospitsky and L. Sonnenschein, *Comput. Phys. Commun.* **148**, 87–102 (2002), [hep-ph/0201292](#).
- [23] E. Richter-Was, D. Froidevaux and L. Poggioli, *ATLFAST 2.0 a fast simulation package for ATLAS*, [ATL-PHYS-98-131](#).
- [24] K. A. Assamagan, Y. Coadou and A. Deandrea, *Eur. Phys. J. direct* **C4**, 9 (2002), [hep-ph/0203121](#).
- [25] K. A. Assamagan and Y. Coadou, *Acta Phys. Polon.* **B33**, 1347–1360 (2002).
- [26] H. L. Lai et al. (CTEQ Collaboration), *Eur. Phys. J.* **C12**, 375–392 (2000), [hep-ph/9903282](#).
- [27] S. Jadach, J. H. Kühn and Z. Was, *Comput. Phys. Commun.* **64**, 275–299 (1990).
- [28] M. Jezabek, Z. Was, S. Jadach and J. H. Kühn, *Comput. Phys. Commun.* **70**, 69–76 (1992).
- [29] S. Jadach, Z. Was, R. Decker and J. H. Kühn, *Comput. Phys. Commun.* **76**, 361–380 (1993).
- [30] D. P. Roy, *Phys. Lett.* **B459**, 607–614 (1999), [hep-ph/9905542](#).
- [31] S. Moretti and D. P. Roy, *Phys. Lett.* **B470**, 209–214 (1999), [hep-ph/9909435](#).
- [32] D. J. Miller, S. Moretti, D. P. Roy and W. J. Stirling, *Phys. Rev.* **D61**, 055011 (2000), [hep-ph/9906230](#).
- [33] B. C. Allanach et al., *Eur. Phys. J.* **C25**, 113–123 (2002), [hep-ph/0202233](#), [[eConf C010630](#) (2001) P125].